Free Radical Biology and Medicine 117 (2018) 247–257

Contents lists available at ScienceDirect

Free Radical Biology and Medicine

journal homepage: www.elsevier.com/locate/freeradbiomed

Selenite and methylseleninic acid epigenetically affects distinct gene sets in myeloid leukemia: A genome wide epigenetic analysis

Prajakta Khalkar[a,1], Hani Abdulkadir Ali[b,d,1], Paula Codó[a], Nuria Díaz Argelich[a,c,e], Anni Martikainen[a], Mohsen Karimi Arzenani[b,d], Sören Lehmann[b,d], Julian Walfridsson[b,d], Johanna Ungerstedt[b,d], Aristi P. Fernandes[a,*]

[a] Division of Biochemistry, Department of Medical Biochemistry and Biophysics (MBB), Karolinska Institutet, SE-171 77 Stockholm, Sweden
[b] Department of Medicine Huddinge, Karolinska Institutet, Stockholm, Sweden
[c] Department of Organic and Pharmaceutical Chemistry, University of Navarra, Irunlarrea 1, E-31008 Pamplona, Spain
[d] Hematology Center, Karolinska University Hospital, Stockholm, Sweden
[e] Instituto de Investigación Sanitaria de Navarra (IdiSNA), Irunlarrea 3, E-31008 Pamplona, Spain

ARTICLE INFO

Keywords:
Selenium
ChIP sequencing
Histone marks
AML
Anticancer agents

ABSTRACT

Selenium compounds have emerged as promising chemotherapeutic agents with proposed epigenetic effects, however the mechanisms and downstream effects are yet to be studied. Here we assessed the effects of the inorganic selenium compound selenite and the organic form methylseleninic acid (MSA) in a leukemic cell line K562, on active (histone H3 lysine 9 acetylation, H3K9ac and histone H3 lysine 4 tri-methylation, H3K4me3) and repressive (histone H3 lysine 9 tri-methylation, H3K9me3) histone marks by Chromatin immunoprecipitation followed by DNA sequencing (ChIP-Seq). Both selenite and MSA had major effects on histone marks but the effects of MSA were more pronounced. Gene ontology analysis revealed that selenite affected genes involved in response to oxygen and hypoxia, whereas MSA affected distinct gene sets associated with cell adhesion and glucocorticoid receptors, also apparent by global gene expression analysis using RNA sequencing. The correlation to adhesion was functionally confirmed by a significantly weakened ability of MSA treated cells to attach to fibronectin and linked to decreased expression of integrin beta 1. A striking loss of cellular adhesion was also confirmed in primary patient AML cells. Recent strategies to enhance the cytotoxicity of chemotherapeutic drugs by disrupting the interaction between leukemic and stromal cells in the bone marrow are of increasing interest; and organic selenium compounds like MSA might be promising candidates. In conclusion, these results provide new insight on the mechanism of action of selenium compounds, and will be of value for the understanding, usage, and development of new selenium compounds as anticancer agents.

1. Introduction

Due to the generally highly proliferative state, tumor cells have an aberrant metabolism and generate more reactive oxygen species (ROS) than normal cells. In response to higher levels of ROS, cancer cells increases their antioxidant capacity, forcing them to maximize their antioxidant capacity and subsequently making them more vulnerable to additional ROS production [1,2]. Thus, the generation of oxidative stress has lately been proven as a potential anticancer treatment. Selenium (Se) is an essential trace element crucial to mammalian cellular and biological functions, such as antioxidant and anti-inflammatory effects [3]. *Per contra*, in excessive amounts Se is toxic and turns into a pro-oxidant with growth inhibiting and cytotoxic properties [3]. In addition, there is a selective uptake of Se in tumors, the first evidence dating back to the 1960s when ^{75}Se-sodium selenite was assessed as a tumor radiotracer, and was shown to accumulate in tumors with a high accuracy [4,5]. Furthermore, it has been shown that Se induces programmed cell death of tumor cells at concentrations that do not influence the growth and viability of normal cells [2]. However, the concentration, chemical form and redox activity of the Se compounds as

Abbreviations: AML, acute myeloid leukemia; ChIP, Chromatin immunoprecipitation; CML, chronic myeloid leukemia; ECM, extracellular matrix; GO, gene ontology; CD29/ITGB1, integrin beta 1; HIP1, huntingtin interacting protein; DAB2, disabled homolog 2; SDC1, syndecan 1; LSC, leukemia stem cells; LUMA, Luminometric methylation assay; MSA, methylseleninic acid; PTM, post-translational modification; ROS, Reactive oxygen species; Se, Selenium

* Corresponding author.
E-mail address: aristi.fernandes@ki.se (A.P. Fernandes).
[1] Authors have contributed equally.

https://doi.org/10.1016/j.freeradbiomed.2018.02.014
Received 11 December 2017; Received in revised form 5 February 2018; Accepted 6 February 2018
Available online 10 February 2018

well as the experimental model used play crucial roles in the efficacy and toxicity of these compounds. Notably, the redox active and organic forms have shown to possess far more promising effects [2,6].

Previous studies have shown specific selenite cytotoxicity in primary leukemic cells, where normal bone marrow or peripheral blood cells were unaffected [7]. In addition, in an *ex vivo* panel of primary AML cells, selenium, in its inorganic form Selenite (SeO_3^{2-}), was shown to be the most efficient drug when compared to conventional cytostatic agents [8]. Selenite has shown cytotoxic effects in several solid tumors as well as hematological malignancies [8,9], unfortunately its significant systemic and organospecific toxic effects has diminished its potential as a drug for clinical use [3]. An early case report, treating an AML patient with high doses of the organic Se form, selenocystine, showed promising results [10]. Another organic Se compound methylseleninic acid (MSA) has shown cytotoxicity in tumors at lower concentrations and with fewer side effects than selenite [3]. The molecular mechanisms underlying the favorable effects of selenium compound therapies are however yet insufficiently understood.

One proposed mechanism, in addition to the pro-oxidative properties of Se compounds, is the induction of epigenetic alterations, by inhibiting HDAC activity and modulating histone marks [11,12]. Selenite and MSA both increase the total protein level of active chromatin mark H3K9ac with a corresponding decrease in the repressive chromatin mark H3K9me3 protein levels in prostate cancer cells [13]. MSA has also been shown to inhibit HDAC activity in diffuse large B-cell lymphoma lines [11] and esophageal squamous cell carcinoma [14]. A recent study reported a decrease of H3K9me3 and increased H4K16ac after MSA treatment in the breast cancer cell line MCF-7, while selenite decreased the latter histone mark [15]. However, these studies did not assess the distribution of active and repressive chromatin marks across the genome or the downstream effects of the compound and resulting effects on target genes and epigenetic factors, and has not been conducted in a leukemic background. There is however, growing evidence of epigenetic aberrations in AML [16,17].

This study was undertaken to explore the genome wide epigenetic alterations caused by the inorganic selenium compound selenite and the organic form MSA, with the aim to increase the knowledge of the specific cytotoxic effects exerted by respective compounds. Here we show for the first time not only how these compounds affect key histone modifications in leukemia cells, but also how selenite and MSA epigenetically provoke different gene sets that are linked to their cytotoxic profile. In addition, new insight on the cytotoxic mechanism of MSA is uncovered, connected to loss of adhesion and epigenetic effects on glucocorticoid receptors.

2. Materials and methods

2.1. Cell culture

Human chronic myeloid leukemia cells - K562, were cultivated in RPMI 1640 medium (Lonza) supplemented with 10% fetal bovine serum (Lonza) and 1% glutamine (Lonza). On the day of the treatment the culture medium was changed to fresh medium to obtain a 0.7×10^6 cells/ml suspension. Primary AML cells from bone marrow of four patients (one male and three females) were sampled at the time of diagnosis. The average age of patients was 62 years and their mean age ranged from 38 to 84 years. Three patients have had the *de novo* AML subtype and the fourth patient had secondary AML. The average number of blasts in the patients was 65.5%. Mononuclear cells were separated using density gradient by Ficoll separation (Lonza) and then vitally frozen. At the time of the experiment cells were thawed, cultured and seeded at a density of 2.2×10^5 cells/ml in RPMI 1640 medium (Lonza) supplemented with 10% fetal bovine serum (Lonza). The cells were treated with 6 μM selenite (Sigma) or 5 μM MSA (Sigma) for 24 h and incubated in a humidified incubator at 37 °C and 5% CO_2. Cell viability was measured using the neutral red assay as well as the MTT assay. Experiments involving human material were approved by the Regional Ethical Committee in Stockholm.

2.2. Nuclear protein extraction and HDAC activity assay

Post treatment, cell pellets were washed with PBS followed by centrifugation for 10 m at 1800 × *g* in 4 °C. A second wash was done using a hypotonic buffer (10 mM HEPES, pH 7.9, 1.5 mM $MgCl_2$, 10 mM KCl, 0.5 mM DTT) supplemented with cOmplete™ Protease Inhibitor Cocktail (Roche) and the suspension was centrifuged again for 5 m at 4 °C (1800 × *g*). The cells were then suspended in the hypotonic buffer and incubated on ice for 10 m. The samples were homogenized by passing the cell suspension 5 times through a 23G syringe and 27G syringe each, before centrifugation for 15 m at 4 °C (3300 × *g*). The nuclear pellets were suspended in a TNM buffer (0.1 M NaCl, 0.3 M sucrose, 10 mM Tris-HCl (pH 7.4), 2 mM $MgCl_2$, 0.5% NonidetP-40, 1% glycerol, 0.5 mM DTT (all from Sigma-Aldrich), cOmplete™ Protease Inhibitor Cocktail (Roche) and incubated on ice for 10 m before sonication for 15 s with an output of 70% with a Microson™ Ultrasonic cell disruptor XL (Misonix). The samples were centrifuged for 10 m at 4 °C (10,000 × *g*) and the supernatants were collected and frozen at − 80 °C. The protein concentration was determined using the Bio-Rad protein assay (Bio-Rad) according to the manufacturer's instructions. The nuclear HDAC activity was determined using the HDAC Activity Fluorometric Assay Kit (BioVision) following instructions from the manufacturer. Trichostatin A and HeLa cell extracts, provided in this kit were used as negative and positive controls respectively according to manufacturer's instructions.

2.3. Luminometric methylation assay (LUMA)

DNA was extracted and purified using the Isolate II Genomic DNA Kit (Bioline) following instructions from the manufacturer. DNA concentration was determined using the Nanodrop 2000 Spectrophotometer (Thermo Fischer Scientific). Genome-wide DNA methylation was assessed using the Luminometric Methylation Assay as described in detail by Karimi et al. [18].

2.4. Western blot

Nuclear extracts containing 20 μg of proteins were separated on a Bolt™ 4–12% Bis-Tris Gel (Novex) and transferred to a nitrocellulose membrane using the iBlot Gel Transfer Device (Invitrogen). Five different primary antibodies were used in separate membrane strips, all of rabbit polyclonal origin and with anti-human histone specificity for: H3 (tri-methyl K9) (ab8988, Abcam), H3 (tri-methyl K4) (AB-001–0024, Diagenode), H3 (acetyl K9) (ab4441, Abcam); total H3 (06–755, Millipore), β- actin (A5441, Sigma-Aldrich). Incubation with primary antibody diluted in TBST containing 3.5% bovine serum albumin (BSA) was done overnight at 4 °C. Secondary antibodies (1:5000 in TBST with 5% dry milk) were incubated for 1 h. Membranes were developed using the Amersham™ ECL™ Start Western Blotting Detection Reagent (GE Healthcare) and bands were visualized using the Bio-Rad Quantity One imaging system (Bio-Rad).

2.5. Chromatin immunoprecipitation (ChIP), sequencing and ChIP-qPCR

K562 cells were collected by centrifugation post treatment, resuspended in PBS and fixed in Formaldehyde (Sigma Aldrich) with 8 m incubation at room temperature. ChIP was performed using the iDeal ChIP-Seq kit set for Histones (AB-001–0024, Diagenode) following manufacturer's instructions. For chromatin shearing, sonication was performed in shearing buffer in 1.5 ml TPX microtubes (C30010010-300, Diagenode) sonicated using the Bioruptor sonicator (B01020001, Diagenode) with 25 sonication cycles. For the magnetic immunoprecipitation 1 μl of ChIP-seq grade control antibody was added

per tube with 100 µl of sheared chromatin corresponding to 1×10^6 cells (same ChIP grade antibodies as for western blot were used). After chromatin decrosslinking the fragmented DNA was purified with the MiniElute PCR Purification Kit (28004, Qiagen) and the DNA concentration was measured using Qubit Fluorometric Quantitation with High Sensitivity (Q32851, Thermo Fischer Scientific). The samples were further used for sequencing and ChIP-qPCR as mentioned below.

The library was prepared using the ThruPLEX DNA-seq Kit (R400428, Rubicon Genomics) following instructions of manufacturer. Once finished, the quality of samples was evaluated with the 2100 Bioanalyzer system (Agilent Technologies) and the library clean up and size selection was done using the Agencourt® AMPure® XP magnetic beads (Qiagen). DNA concentration was measured using Qubit and up to 6 samples with different barcodes per lane were pooled to a maximum concentration of 1 ng/µl. 7 pmol of each library with 1% PhiX, was hybridized to the flow cell. Clusters were generated with the cBot, and the flow cell was sequenced on the Illumina HiSeq. 2000 with single end sequencing. As a primary quality control of the sequencing the intensities and base calling parameters were checked (using default parameter settings) with the HiSeq Control software, followed by demultiplexing of the libraries.

2.6. Bioinformatic analysis

The raw sequencing reads in FASTQ format were quality control checked with the FASTQC tool (version 0.11.4) (Babraham Bioinformatics), and eventual adapter sequences and duplicates were removed in order to get at least 10×10^6 filtered reads. The filtered data was then mapped using Bowtie (version 2.2.6) to the human reference genome issue HG-19 (https://www.ncbi.nlm.nih.gov/grc/human/issues/HG-19), with the requirement of unique alignment. Bedgraphs were generated using BED tools (version 2.16.2) and the data was visualized as custom tracks with the UCSC genome browser (https://genome.ucsc.edu). Peakcalling was performed with HOMER (version 4.8) (http://homer.salk.edu.homer/) to determine enrichment over the input samples across the whole genome. Peak size for narrow peaks was set to 150 bp, and 500 bp for broad peaks. The enriched regions were then annotated to the closest transcription start site using HOMER, and differential analysis between treated and control samples was performed with edgeR (version 3.14.0) (Bioconductor). As a cut off for further downstream analysis a logarithm of fold change (log FC) greater than or equal to 2, and log FC less than or equal to −2 was used.

2.7. RNA sequencing

Post treatment, RNA was extracted and purified from K562 cells using the RNeasy Plus Mini Kit (Qiagen) with on column DNase digestion according to manufacturer's instructions. RNA concentration was determined using the Nanodrop 2000 Spectrophotometer (Thermo Fischer Scientific). The experiment was performed in three biological replicates. RNA-Sequencing, to reveal the presence and quantity of the entire transcriptome, after MSA treatment, was performed at the Beijing Genomics Institute (BGI), China, and surveyed in a very high-throughput and quantitative manner at single-base resolution. The RNA-Sequencing was executed with the BGISEQ-500 sequencing system.

2.8. Quantitative polymerase chain reaction (qPCR)

Following RNA extraction, first strand cDNA was generated by reverse transcription using the Thermo Scientific Maxima First Strand cDNA Synthesis Kit for RT-qPCR (Thermo Fischer Scientific), using 1 µg template RNA according to the protocol provided by the manufacturer. All the qPCRs were performed in duplicates on 96-well plates using a PikoReal Real-Time PCR System (Thermo Fischer Scientific) and Luminaris Color HiGreen Master Mix (Thermo Fischer Scientific). The final reaction volume was 10 µl and contained 0.1 µl of cDNA per reaction. Refer Supplementary information for primer sequences. All primer pairs had an efficiency of 100% +/−5%. The PCR program used was 50 °C 2 min, 95 °C 2 min, 95 °C 15 s and 60 °C 30 s (40 cycles). Results were analysed using the $2_T^{-\Delta\Delta C}$ method, and β-actin was used as endogenous control.

For ChIP-qPCR, purified DNA obtained after the ChIP was used as template (150 ng DNA per reaction) and amplified for target genes as mentioned above. Enrichment for H3K9Ac was validated by qPCR with primers specific for the target genes in their promoter regions and the expression was normalized to percentage of input sample, that is a part of the sample not subjected to ChIP.

2.9. Flow cytometry

Post treatment, 5×10^5 cells were incubated with CD29 (integrin β1, ITGB1) (FITC conjugate, clone MEM-101A, Thermo Fischer Scientific), for 30 m at 4 °C in the dark. Cells were fixed in 1% paraformaldehyde at 4 °C and analysed on a FACSCanto II (BD Biosciences) flow cytometer. The data were analysed using FlowJo software (Treestar).

2.10. Adhesion assay

K562 and AML cells at a density of 7×10^5 cells/ml were treated with MSA 5 µM or vehicle for 24 h and 20 h respectively. The adhesion assay was performed with a modified procedure described by Damiano et al. [19]. Briefly, a human fibronectin coated 96 well plate (Corning) was blocked for one hour at room temperature with 1% BSA. Wells were washed once with serum-free RPMI 1% glutamine and 50,000 cells were added per well and allowed to attach for 3 h at 37 °C. After the incubation, wells were washed three times with medium to remove unattached cells. Adherent cells were then fixed with 70% methanol for 10 m and incubated with a 0.5% crystal violet 20% methanol solution for additional 10 m and washed with water. Absorbance was read at 590 nm.

2.11. Statistics analysis

All numerical data are presented as a mean of three independent experiments unless otherwise stated. Statistical analyses were performed using GraphPad PRISM software. Students's '*t*-test' was applied to the data obtained and *P* values less than 0.05 were considered statistically significant. The statistical methods used, for the bioinformatics, in the differential analysis are multi-group statistical testing developed by Robinson and Smyth [20,21].

3. Results

3.1. Global effects of selenite and MSA on epigenetic marks

Based on viability titration experiments, 6 µM of selenite and 5 µM of MSA were chosen to achieve moderate toxicity in all experiments (approximately 20% cell death after 24 h treatment) (Fig. 1A). As a control to check the specificity of these compounds towards the tumor cells, human buffy coat from five healthy donors were treated with 10 µM of selenite or MSA for 24 h, and no significant cell death was observed after treatment with neither of the two compounds (Control: 100% viability ± 9 std.dev, Selenite: 89% viability ± 17 std.dev, MSA: 97% viability ± 16 std.dev). The epigenetic alterations in K562 cells were examined on a global level in terms of alterations of total nuclear HDAC activity, which upon 24 h treatment showed a tendency to decreased approximately 10% with selenite and MSA respectively (Fig. 1B). However, these results were not statistically significant. In order to determine the potential impact of the two selenium compounds on total genomic DNA methylation, the LUMA technique was used, but

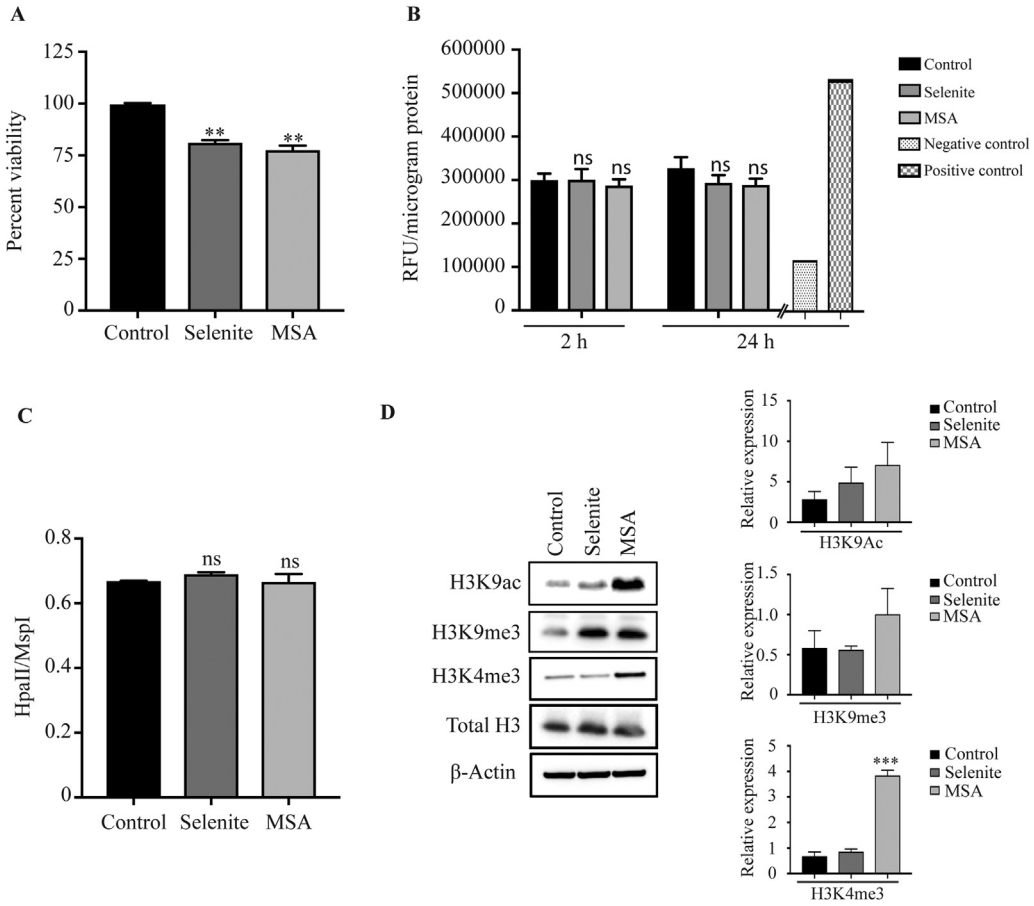

Fig. 1. Epigenetic effects of selenite and MSA on K562 cells. A) Cell viability, determined by neutral red assay, after treatment for 24 h with 5 μM selenite or 6 μM MSA. B) Nuclear HDAC activity after incubation with selenite or MSA for 2 or 24 h. Trichostatin A and HeLa cell extracts were used as negative and positive controls respectively. C) Global DNA methylation determined by LUMA, after incubation with selenite or MSA for 24 h. D) Western blot analysis of H3K9ac, H3K9me3 and H3K4me3 after treatment with selenite (S) or MSA (M) for 24 h (representative figure out of three independent experiments). Graphs show quantification of H3K9ac, H3K9me3 and H3K4me3 proteins normalized by beta-actin. Selenite and MSA treated samples were compared to the control and the levels of significance were calculated using *t*-test for independent samples (ns: non-significant, $^{**}p \leq 0.01$, $^{***}p \leq 0.001$). Data presented represents the mean out of at least three independent experiments.

again no significant changes were observed (Fig. 1C). Previous studies have shown that Se compounds modify histones via post-translational modifications (PTMs) on a global level, detecting acetylated and methylated histone proteins by western blot in different cell lines [13,22]. Therefore, the effects of selenite and MSA on the occurrence of specific acetylation and methylation sites on H3K4me3, H3K9me3 and H3K9ac were studied using Western Blot. The results displayed that after 24 h the active histone mark, H3K4me3 was strongly upregulated upon MSA treatment and H3K9ac as well as H3K9me3 showed a clear tendency of enrichment. However, selenite treatment did not significantly alter these histone marks (Fig. 1D).

3.2. Genome wide changes in active and repressive histone marks upon MSA and selenite treatment

ChIP followed by whole genome sequencing was performed using antibodies against active (H3K9ac, H3K4me3) and repressive (H3K9me3) histone marks, after 24 h treatment of cells with selenite or MSA. ChIP sequencing data was assessed after defining peak size as 150 bp for H3K9ac and H3K4me3, and 500 bp for H3K9me3. Peaks annotated were 5386 of 65242 for H3K9ac, 5382 of 60685 peaks for H3K4me3 and 683 of 82781 peaks for H3K9me3. In a first evaluation of the results, the data were selected based on a two log fold change (log2FC) between the control and treated samples, after subtraction of the input of each sample.

The global effects on number and partial overlap of protein coding genes affected by selenite and MSA are illustrated with Venn-diagrams (Fig. 2A). Overall, MSA induced changes in histone modifications in a larger number of genes compared to selenite however, for both active and repressive histone marks, there are sites of increased as well as decreased enrichments of the respective histone mark. While roughly half of the genes affected by selenite overlap with MSA (H3K9ac), the majority of the genes affected by MSA display no overlap with selenite.

The difference in overall changes of histone modifications between the two compounds is visualized in heat maps (Fig. 2B-C), were the genes with the highest or lowest log FC after MSA treatment are illustrated for H3K9ac. The genes that show the highest change in enrichment for MSA were barely affected by selenite, and selenite instead showed histone modification patterns similar to the control sample. Similar patterns are seen for H3K9me3 and H3K4me3 (Supplementary Fig. 1).

3.3. ChIP sequencing data analysis

The log2FC compared to control was used as criteria for the gene ontology (GO) analysis, including both up- and downregulated genes and ranked according to fold change. Listed in Table 1 are the GO pathways of molecular functions and cellular components that have been significantly affected by MSA for H3K9ac. In Fig. 3, a graphical overview of significantly enriched GO pathways (from Table 1) after MSA treatment are illustrated, and display a clear effect on cell adhesion, as well as glucocorticoid receptor binding and Inositol-3-phosphate synthase activity. The GO terms of biological processes significantly affected by MSA for H3K4me3 are listed in Supplementary Table 1, wherein the most pronouncedly affected categories were connected to cell adhesion. These adhesion categories remained unaffected by selenite after 24 h of treatment and therefore seem to be very specific MSA effects.

As selenite is known to trigger oxidative stress by generation of ROS, with the consequence of upregulating the expression of genes that can counteract the effect [8,23], logFC > 2 was selected for GO analysis to explore if an increase in enrichment was evident epigenetically as well. Only H3K9ac had significantly altered peaks to display significant changes in GO, but it is clear that the biological processes affected by

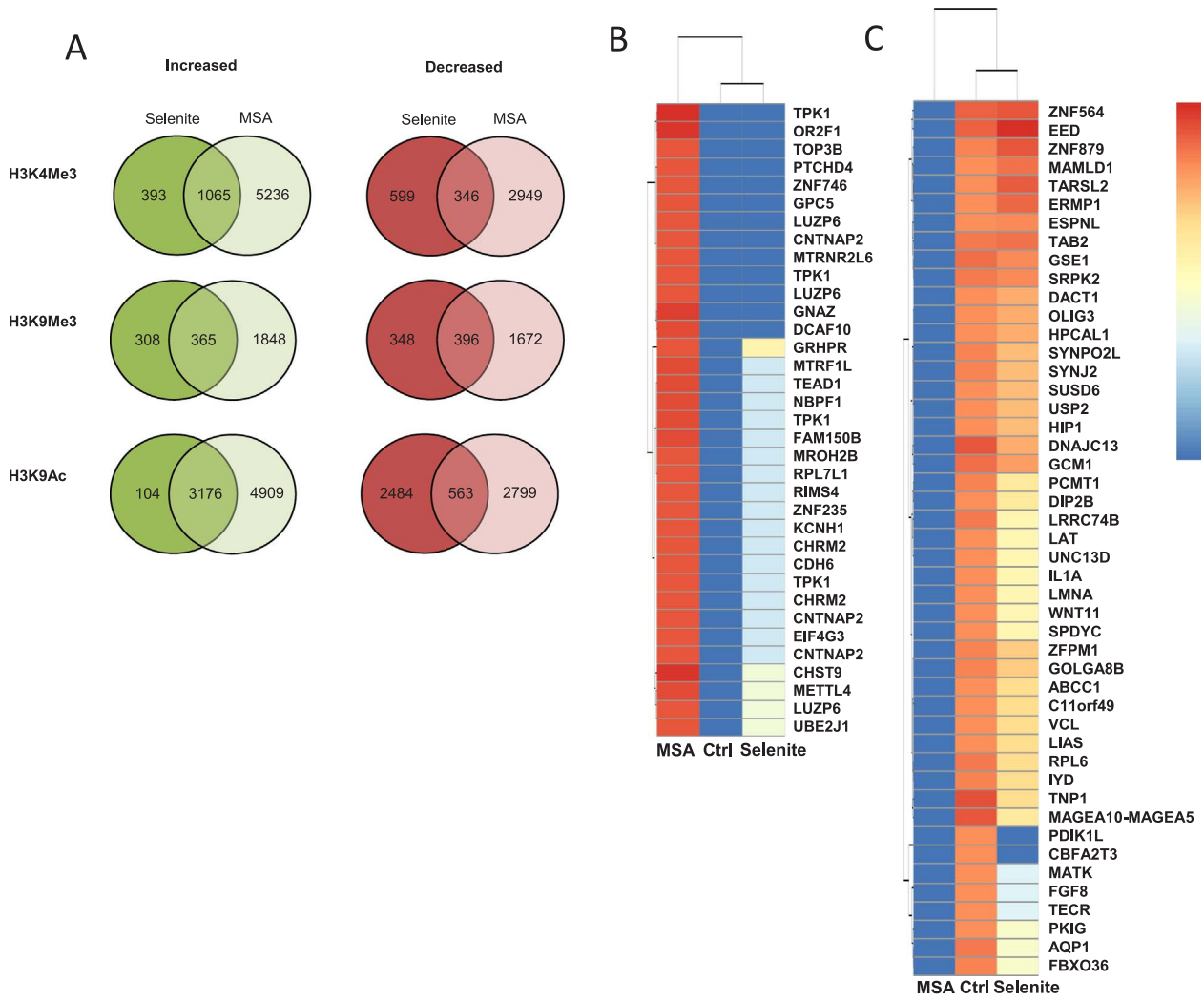

Fig. 2. Genome wide alterations on histone marks by selenite and MSA in K562 cells. A) Venn diagrams illustrating the number of significant alterations in enrichments of protein coding regions, and the overlap between selenite and MSA treatment. B-C) Heat maps illustrating the highest changes in enrichment (both increased and decreased) for H3K9ac protein coding genes with MSA treatment compared to control and selenite. B) logFC > 2 (35 genes) and C) logFC < −2 (47 genes).

selenite for H3K9ac to a high degree represent responses to oxygen and hypoxia (Table 2).

3.4. Analysis of RNA sequencing after MSA treatment

In order to explore the downstream effects of the chromatin modifications caused by MSA, the RNA transcriptome of the same samples were sequenced and quantified. Differentially expressed genes (DEGs) were screened using Possion Distribution method in order to perform further functional analysis. As a cut off for downstream analysis a log FC ≥ 2 and log FC ≤ -2 was set. Also, correction of p-value corresponding to DEGs was performed using Bonferroni method and corrections for false positives and false negatives errors were performed using the FDR method. FDR value ≤ 0.001 and absolute value of log2Ratio ≥ 1 was set as threshold to judge the significance of DEGs. Fig. 4 illustrates the total number of genes that have been significantly up or downregulated by MSA (Fig. 4A) and Selenite (Fig. 4B). Amongst the two, MSA displays more pronounced DEGs (979 up and 470 downregulated) as compared to Selenite (27 up and 18 downregulated). Further GO analysis was performed on the DEGs, both up and downregulated, after MSA treatment and a graphical overview of significantly enriched GO terms with molecular functions is shown in Fig. 4C. In concordance to the ChIP sequencing results (Fig. 3), the GOs significantly altered by MSA observed after RNA sequencing are the categories related to cellular binding and adhesion (Fig. 4C). A comparative study of significantly enriched GOs after MSA treatment obtained by both RNA- and ChIP- sequencing (H3K9Ac) analysis was performed and illustrated in Fig. 4D.

Genes such as CD29, disabled homolog 2 (DAB2), huntingtin interacting protein 1 (HIP1), syndecan 1 (SDC1), leukocyte differentiation antigen (CD84) and tetraspanin 29 (TSPAN29, CD9), linked to cellular adhesion, were found to be differentially regulated after MSA treatment as observed in both RNA- and ChIP- sequencing (H3K9Ac) analysis (Fig. 4C and D). Further, in order to validate our findings and study the early cytotoxic effects, a ChIP-qPCR with active chromatin mark H3K9Ac was performed after 3, 6 and 24 h of MSA treatment. The genes DAB2 and HIP1 are significantly downregulated (H3K9Ac decreased) after 3 h of treatment and the CD29 is significantly downregulated after 6 h of treatment (Fig. 5A). Also, mRNA expression of these genes was examined by qPCR after 6 h and 24 h of MSA treatment. The levels of CD29, DAB2, HIP1 and CD9 mRNA after 6 h of MSA treatment were significantly decreased whereas the CD84 and SDC1 showed significant increase their mRNA expression (Fig. 5B). Apart from DAB2, selenite did not show any significant changes in mRNA expression of these genes (Fig. 5B). The transient effect observed at 6 h reflects that it is an early event, preceded by histone alterations, and might be involved in the cytotoxic effects caused by MSA, and reinforce the findings that selenite and MSA have different mechanism of action.

Table 1
Molecular functions and cellular components significantly affected by MSA for H3K9ac (log2FC).

Molecular functions			
GO term	**Description**	**P-value**	**FDR q-value**
GO:0045296	cadherin binding	2.09E−5	7.07E−2
GO:0035257	nuclear hormone receptor binding	3.28E−5	5.55E−2
GO:0098641	cadherin binding involved in cell-cell adhesion	4.23E−5	4.77E−2
GO:0035259	glucocorticoid receptor binding	5.66E−5	4.78E−2
GO:0098632	protein binding involved in cell-cell adhesion	6.78E−5	4.58E−2
GO:0098631	protein binding involved in cell adhesion	9.21E−5	5.19E−2
GO:0019899	enzyme binding	9.61E−5	4.64E−2
GO:0050839	cell adhesion molecule binding	1.4E−4	5.91E−2
GO:0035258	steroid hormone receptor binding	2.16E−4	8.1E−2
GO:0046915	transition metal ion transmembrane transporter activity	2.66E−4	8.98E−2
GO:0051427	hormone receptor binding	4.71E−4	1.45E−1
GO:0004512	inositol−3-phosphate synthase activity	8.75E−4	2.46E−1
GO:0016872	intramolecular lyase activity	8.75E−4	2.27E−1

Cellular component			
GO term	**Description**	**P-value**	**FDR q-value**
GO:0005737	cytoplasm	1.29E−4	1.88E−1
GO:0005913	cell-cell adherens junction	1.59E−4	1.16E−1
GO:0005912	adherens junction	5.45E−4	2.66E−1
GO:0070161	anchoring junction	7.53E−4	2.75E−1

Other DEGs connected to cell adhesion that were significantly affected in the ChIP sequencing analysis but not in the RNA sequence analysis, were also investigated by qPCR after 6 and 24 h of treatment. As seen in Fig. 5C all three genes examined (MET, RICTOR and ZEB1) show clear increase in mRNA level after a 6 h of treatment with MSA but not after selenite treatment thus confirming the ChIP sequencing results.

3.5. Adhesion analysis based on ChIP sequencing data

To explore if the enrichment found from the ChIP sequencing by MSA is translated into functional changes, adhesion properties of K562 cells were investigated after treatment with MSA. One gene that is of great importance in the adhesion of hematopoietic cells to the extracellular matrix (ECM), and that was found to have an altered enrichment for H3K9ac after MSA treatment, was CD29. The peaks from the promoter region for CD29 for active chromatin marks H3K9ac and H3K4me3 in the ChIP sequencing data (Fig. 6A) displayed a clear decrease upon MSA treatment. CD29 was confirmed to be significantly decreased after 24 h treatment with MSA by flow cytometry (Fig. 6B). Furthermore, to establish whether this decrease in CD29 truly had an effect on the cell's ability to attach to a surface, adhesion analysis was performed, and revealed that cells treated with MSA had a significant impaired ability to adhere onto the fibronectin coated plate (Fig. 6C). The loss of adhesion after MSA treatment was also confirmed using primary AML cells derived from the bone marrow of 4 different patients. In the primary cells a 45% loss in adhesion was observed following MSA treatment without significantly affecting the cell viability (Control: 100% viability ± 13.0 std. dev, Selenite: 85.04% viability ± 9.8 std. dev, MSA: 97.95% viability ± 5.1 std. dev) (Fig. 6D).

4. Discussion

The purpose of this study was to examine the role of genome wide epigenetic changes in the cytotoxic mechanism of action of the inorganic selenite and organic MSA. The initial findings from the ChIP sequencing showed not only that the compounds had caused profound histone modifications, but also that there seemed to be large differences between selenite and MSA. The Venn-diagrams show that MSA affects a larger number of genes and that many are specific for this compound. The distinct effects of the two compounds are also evident in the heat maps and in the GO analyses. Selenite, which is well known to mediate its cytotoxic effect through generation of ROS [24], mainly superoxide, had a significant enrichment of H3K9ac of genes within the GO terms for biological processes for oxygen response and hypoxia, as expected. Despite K562 cells being p53 negative, which has been shown to inhibit the cytotoxic effect of selenite in AML cells [25], ROS dependent cytotoxic effects in K562 by selenite has been previously reported. In the aforementioned study, a correlation between toxicity caused by ROS generation after selenite treatment and induction of topo II-DNA complexes was observed. These effects were shown to occur in a time-dependent manner and correlated with the induction of apoptosis [26].

The cytotoxic effects exerted by MSA are in contrarily not solely mediated by superoxide or hydrogen peroxide but suggested to be via a different mechanism [27]. Our results, showing that the GO enrichment sites obtained for MSA are almost completely different from the ones obtained for selenite, strengthen these results. The GO analysis of our ChIP sequencing data revealed very relevant and specific effects of MSA on genes sets connected to cell adhesion and glucocorticoid receptor binding. The latter being very interesting as Prasad et al. recently reported a homozygote mutation of the selenoprotein thioredoxin reductase 2 in humans giving rise to glucocorticoid deficiency [9].

The effect of MSA on adhesion might have a clinical relevance as the interaction between leukemic cells and bone marrow stroma plays a vital role in both the prognosis of leukemia and of the development of drug-resistance of leukemic cells [28]. A plausible explanation is that leukemia stem cells (LSC) can be dormant in the bone marrow niche [29] taking advantage of this rich and protective environment to escape from chemotherapeutic treatments [30,31]. This is also an important cause of the poor efficacy of some targeted leukemia stem cell therapies [32–34]. Therefore, understanding and finding new ways to disrupt the interaction of leukemic cells and stromal cells, as an approach to enhance the cytotoxicity of chemotherapeutic drugs is of utmost interest. In a study by Garrido et al., direct contact with human bone marrow stromal cells reduced drug-induced apoptosis of AML cells [35]. Causing these LSCs to detach from the bone marrow could therefore make them more vulnerable to chemotherapy.

The most relevant adhesion molecules as of now include CD44, integrins and selectins. In our data set CD29, one of the protein coding genes with altered enrichment caught our attention. The altered enrichments of CD29 also translated down to protein level, and had a significant effect on the adhesion of cells to fibronectin. Maybe even more importantly, the same finding, with loss of adhesion, was also observed in human primary AML cells from the bone marrow, strongly indicating that MSA might contribute to the detachment of cells from the ECM in the bone marrow. Recently, the critical role of integrins in minimal residual disease (MRD) persistence and LSC homing has been further strengthened by observations where overexpression of α6 and β4 integrins enhanced drug resistance by increasing laminin adhesion of EVI1 positive AML cells [36]. Due to the role of integrins in homing of lymphoid tumor cells to their metastatic sites, integrin targeting in LSCs might theoretically also be an approach to prevent colonization of organs by leukemic cells [37]. The effect on adhesion and integrins by MSA is also well connected to previous reports showing the significant effect of MSA on calcium ion signaling and calcium channel activity, as increase of intracellular Ca^{2+} levels stimulated by integrin-mediated adhesion have been demonstrated [38,39]. The connection between Ca^{2+} and adhesion caused by MSA requires further studies to understand the exact mechanism of action, especially considering that the calcium dependent cadherins were also found to be epigenetically affected. It is well documented that MSA has suppressive effects on

Fig. 3. Graphical overview of significantly enriched GO categories after MSA treatment (log2FC) in K562 cells. A) Molecular functions and B) Cellular components. A child node represents a more specific instance of a parent node, to which it is connected with. Red boxes represent significantly enriched GO categories and black boxes represent non-enriched GO categories that are included in the graph to allow tracing of the interrelationships between the GO categories.

Table 2
Biological process significantly affected by selenite (logFC > 2) for H3K9ac.

GO term	Description	P-value	FDR q-value
GO:1900101	regulation of endoplasmic reticulum unfolded protein response	3.7E−5	3.14E−1
GO:1903894	regulation of IRE1-mediated unfolded protein response	1.11E−4	4.7E−1
GO:0055010	ventricular cardiac muscle tissue morphogenesis	1.55E−4	4.38E−1
GO:1900102	negative regulation of endoplasmic reticulum unfolded protein response	1.78E−4	3.79E−1
GO:0001666	response to hypoxia	2.93E−4	4.99E−1
GO:0036293	response to decreased oxygen levels	4.01E−4	5.69E−1
GO:0070482	response to oxygen levels	5.23E−4	6.36E−1
GO:1903573	negative regulation of response to endoplasmic reticulum stress	6.13E−4	6.51E−1
GO:0007569	cell aging	6.66E−4	6.29E−1
GO:0032461	positive regulation of protein oligomerization	8.04E−4	6.84E−1

phospho-Akt (Ser473) expression, and that in the presence of a calcium chelator or a specific inhibitor of calcineurin (a calcium-dependent phosphatase), this effect is greatly reduced [40].

CD9, a tetraspanin protein, has been implicated in various physiological processes like motility, adhesion and fertilization [41] and plays a critical role in tumor progression and metastasis [42–44]. Several lymphoblastic leukemia's can be distinguished on the basis of their CD9 expression [45,46]. Also it has been shown that CD9 upregulates the adhesion of B leukemic cells to fibronectin and the migration of these cells in response to CXCL12, through a RAC1 dependent pathway, further suggesting a possible key role in late relapse of B acute lymphoblastic leukemia through its effects on migration and homing. [47]. These findings are in concordance with our study wherein we find that both the CD9 and CD29 are downregulated upon MSA treatment and further affects the adhesion of human chronic myeloid leukemia cells as well as primary AML cells.

Additional genes related to cell-cell and/or cell-matrix adhesion and regulation of CD29 such as DAB2 [48,49], HIP1 [50,51], SDC1 [52] were significantly regulated by MSA treatment via PTMs and/or mRNA expression, but their protein levels and activity needs to be further examined. DAB2 has for example been suggested as a putative tumor suppressor, and its expression is downregulated in various tumor cells and it inhibits cell proliferation by inhibiting growth factor signaling [53] However, DAB2 has been shown to affect migration, by promoting TGF beta induced gene expression of VEGF and FGF2 in cancer cells [54,55], suggesting that DAB2 can also promote cancer progression. DAB2 has also shown to regulate cell-cell and cell-fibrinogen adhesion, integrin αIIbβ3 activation and positive regulation of fibrinogen uptake [56,57]. Our results show that MSA treatment significantly decreased the DAB2 expression and therefore might have further lead to loss of cell-cell and/or cell- matrix adhesion.

HIP1, first implicated in cancer biology as a part of chromosomal translocation in leukemia, is a cofactor in clathrin- mediated vesicle trafficking and a key player in cell migration [58]. Clathrin light chain (CLC)- HIP1 interactions are needed for recycling of active CD29 and necessary for cell migration [50]. In addition, HIP1 has been shown to mediate CD29 turnover following c-met activation [51]. In this study,

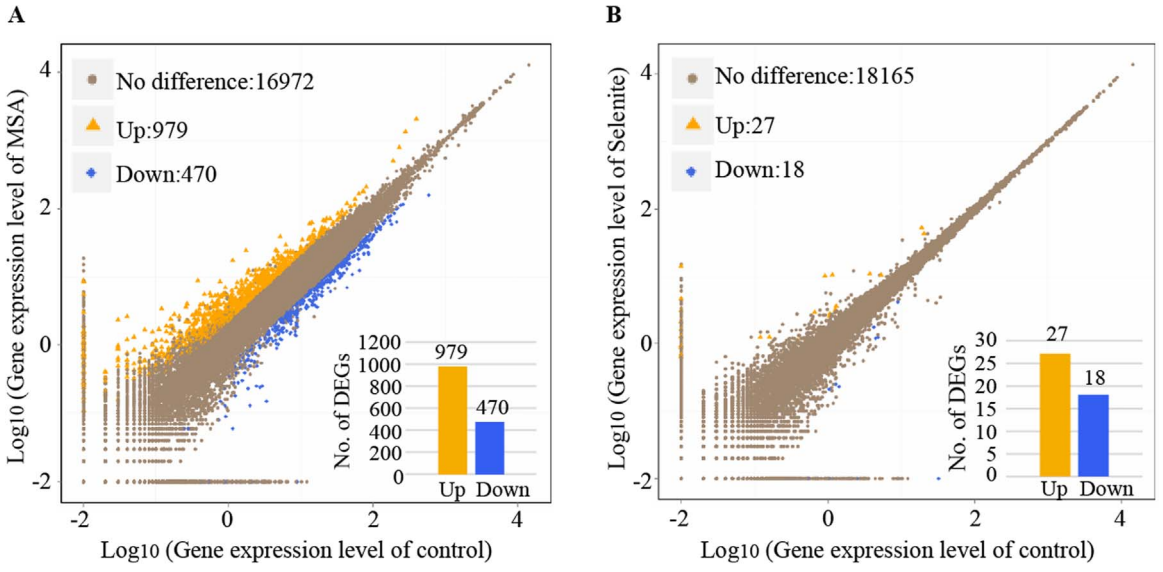

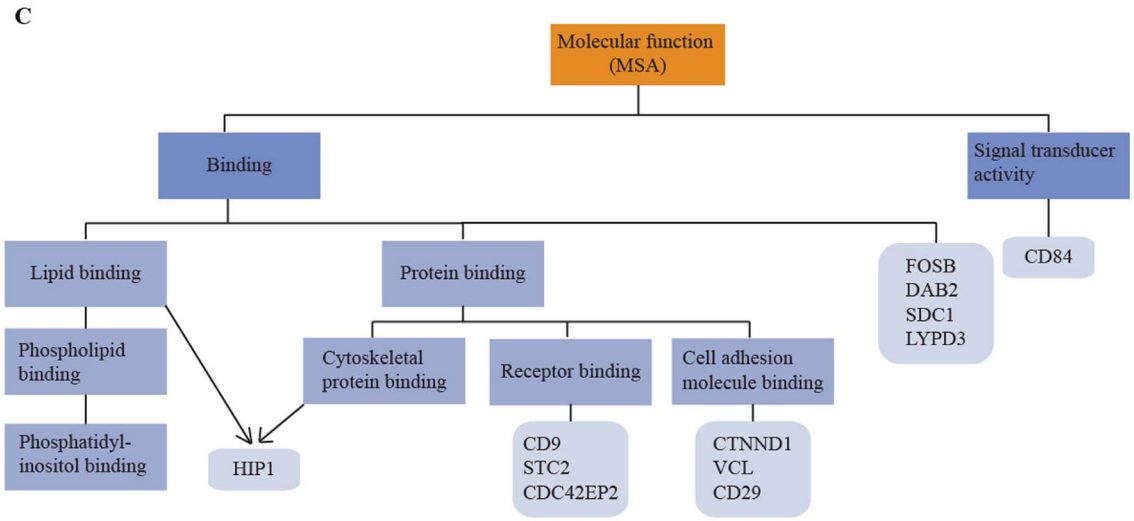

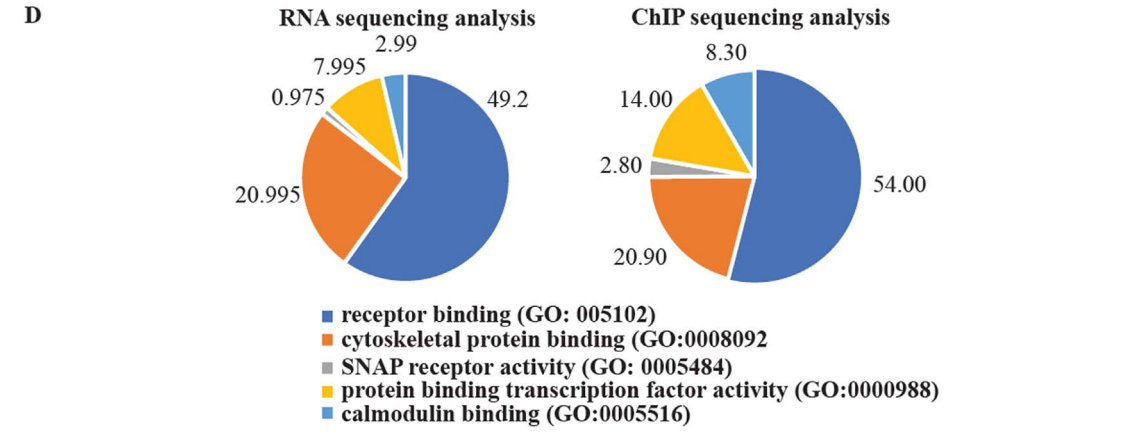

Fig. 4. Alterations on the RNA transcriptome in K562 cells. Number of differentially expressed genes (DEGs) upon treatment with MSA (A) and Selenite (B) as obtained by RNA sequencing analysis. C) Molecular functions altered by MSA treatments. D) Pie-chart comparing the GOs that are significantly regulated after MSA treatment as determined in RNA and ChIP sequencing analysis.

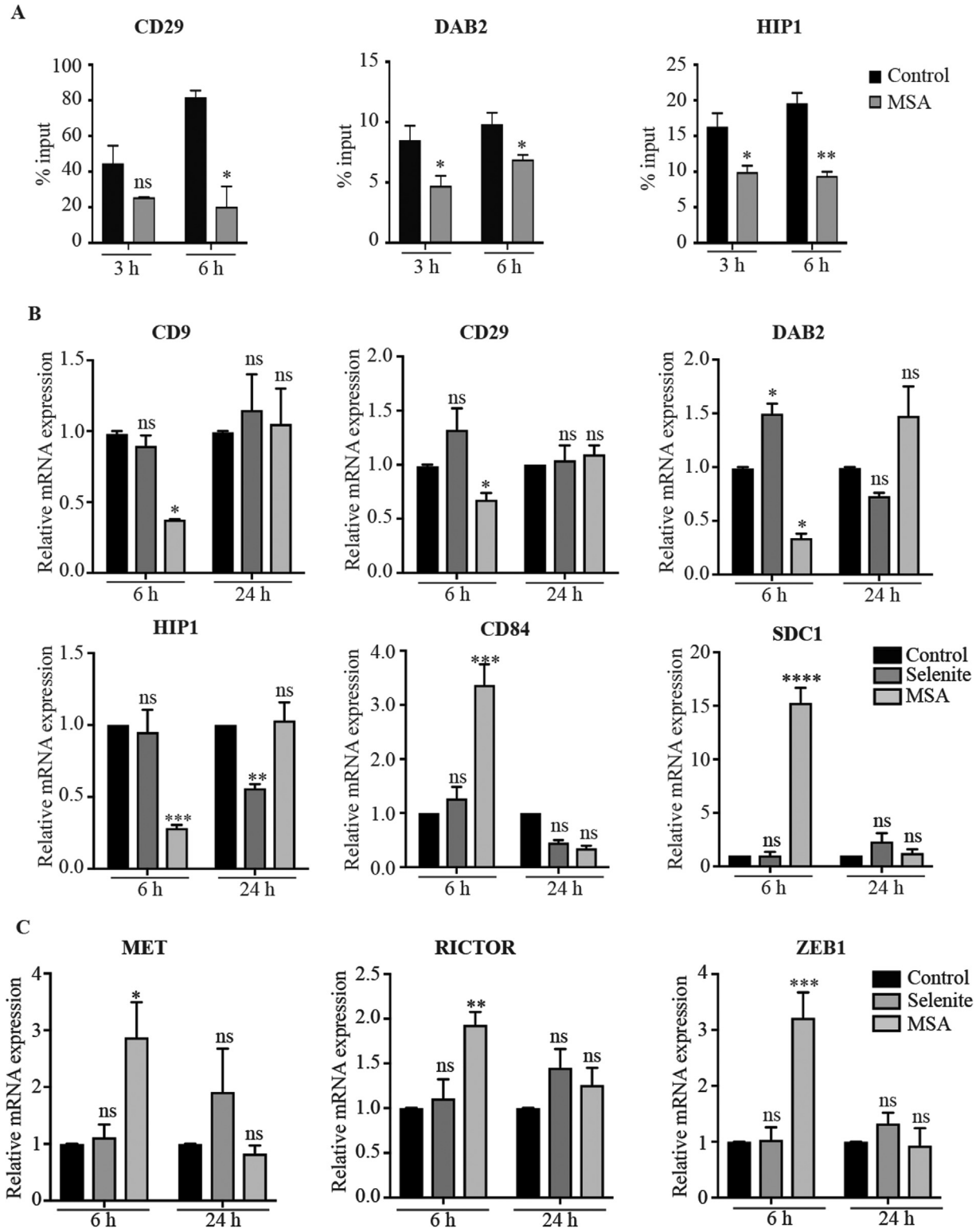

Fig. 5. Expression Analysis of DEGs in connection to adhesion of K562 cells, significantly enriched by MSA. A) Expression of ITGB1/CD29, DAB2 and HIP1 after MSA treatment for 3, 6 and 24 h, as observed in ChIP-qPCR. B) Relative mRNA expression of the DEGs. C) Genes that were significantly changed as observed in ChIP sequencing analysis but not in RNA sequencing analysis. MSA and/or selenite treated samples were compared to the control and the levels of significance were calculated using *t*-test for independent samples (ns: non-significant, *$p \leq 0.05$, **$p \leq 0.01$, ***$p \leq 0.001$, ****$p \leq 0.0001$). B-E represents the mean out of at least three independent experiments.

we found that MSA downregulates the expression of HIP1 which partly might explain the decrease in CD29 expression. SDC1, significantly affected by MSA, has been found to be dysregulated in several cancer forms where altered expression is connected to cancer progression (37). RICTOR-mTOR, herein also significantly affected by MSA via both PTMs and mRNA expression, was previously shown to be required for AKT Ser473 phosphorylation. AKT Ser473 phosphorylation in turn, significantly contributes to CD29 mediated anchoring dependent survival of cells [59,60]. The suppressive effect of MSA on Ser473 phosphorylation might therefore possibly be via the epigenetic alterations of

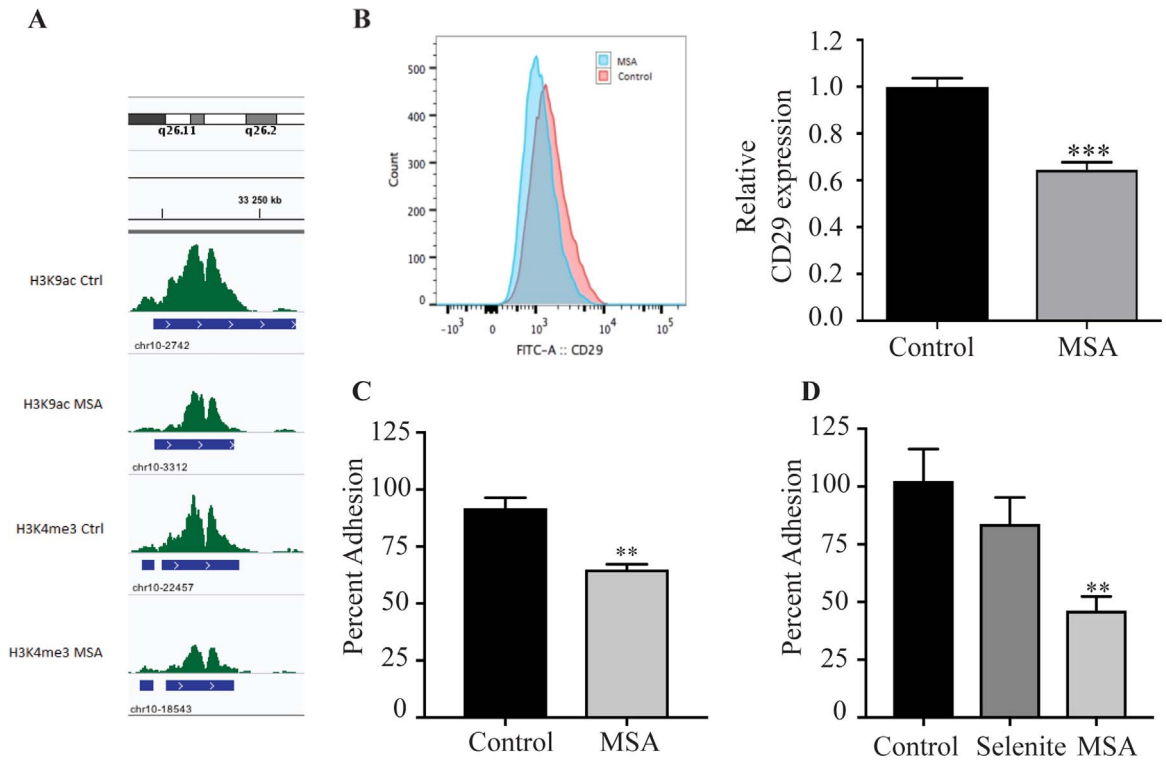

Fig. 6. Effects on adhesion from MSA treatment on K562 and primary AML cells. A) Peak analysis of the promoter region of ITGB1/CD29 for H3K9ac and H3K4me3 after MSA treatment in K562 cells. B) Protein expression of ITGB1/CD29 determined by flow cytometry analysis after 24 h of treatment with 5 μM MSA in K562 cells. C) Adhesion assay, measuring the number of cells attached to fibronectin after 24 h of treatment with 5 μM MSA in K562 cells. D) Adhesion measurements of primary AML cells. (ns: non-significant, *p ≤ 0.05, **p ≤ 0.01, ***p ≤ 0.001, ****p ≤ 0.0001). B-E represents the mean out of at least three independent experiments.

RICTOR. Overall, the findings from the ChIP sequencing translated well to the genes examined on both protein and mRNA levels, and the effect observed at the mRNA level occurred at a relative early time point, prior to any signs of cell death. This indicates that the effects observed on gene expression after MSA treatment at least partially could be explained via histone PTMs.

5. Conclusions

Our study shows that selenium compounds – MSA and selenite affect histone modifications on a global level in a distinct way. Selenite mainly affected pathways involving oxygen and hypoxia responses, while MSA affected adhesion and migration pathways. Further studies are needed to elucidate whether these are direct or indirect epigenetic effects. Nevertheless, it is the first study undertaken to explore the genome wide epigenetic effects of these selenium compounds, and will hopefully lay ground for exploring the anti-carcinogenic effects of these compounds further. Targeting adhesion proteins with MSA might help in detaching the leukemia stem cells from the bone marrow and subsequently overcoming the resistance phenotype in combination therapy with other conventional cytostatic agents.

DeclarationEthical approval

Experiments involving human material were approved by the Regional Ethical Committee in Stockholm (2010/1893-31), with a statement of consent from all participants, and conducted in accordance with the Declaration of Helsinki.Conflict of interests

The authors declare that they have no conflict of interests.Funding

This article has been financially supported by The Swedish Cancer Society (Cancerfonden), Åke Wibergs stiftelse, Stockholm Cancer Society and Marianne and Marcus Wallenbergs foundation. NDA received the pre-doctoral and mobility scholarship from Asociación de Amigos de la Universidad de Navarra.Author contribution

PK performed FACS, Adhesion and ChIP-qPCR experiments, RNA sequencing analysis, statistically analysed data, prepared figures and helped in writing of the manuscript. HA did the bioinformatics and statistical analysis, PC performed WB and experiments sent for ChIP sequencing. NDA, AM and MKA performed experiments and analysed results. SL and JW provided patient material and helped in drafting the manuscript. JU and APF designed and planned the experiments and had the main responsibility in writing the manuscript.

Appendix A. Supporting information

Supplementary data associated with this article can be found in the online version at http://dx.doi.org/10.1016/j.freeradbiomed.2018.02.014.

References

[1] R.A. Cairns, I.S. Harris, T.W. Mak, Regulation of cancer cell metabolism, Nat. Rev. Cancer 11 (2) (2011) 85–95.
[2] G. Nilsonne, et al., Selenite induces apoptosis in sarcomatoid malignant mesothelioma cells through oxidative stress, Free Radic. Biol. Med. 41 (6) (2006) 874–885.
[3] A.P. Fernandes, V. Gandin, Selenium compounds as therapeutic agents in cancer, Biochim. Biophys. Acta 1850 (8) (2015) 1642–1660.
[4] R.R. Cavalieri, K.G. Scott, E. Sairenji, Selenite (75Se) as a tumor-localizing agent in man, J. Nucl. Med. 7 (3) (1966) 197–208.
[5] R.R. Cavalieri, K.G. Scott, Sodium selenite Se 75. A more specific agent for scanning tumors, J. Am. Med. Assoc. 206 (3) (1968) 591–595.
[6] C.M. Weekley, H.H. Harris, Which form is that? The importance of selenium speciation and metabolism in the prevention and treatment of disease, Chem. Soc. Rev. 42 (23) (2013) 8870–8894.
[7] X.R. Jiang, et al., The anti-leukaemic effects and the mechanism of sodium selenite, Leuk. Res. 16 (4) (1992) 347–352.
[8] E. Olm, et al., Selenite is a potent cytotoxic agent for human primary AML cells, Cancer Lett. 282 (1) (2009) 116–123.
[9] R. Prasad, et al., Thioredoxin Reductase 2 (TXNRD2) mutation associated with familial glucocorticoid deficiency (FGD), J. Clin. Endocrinol. Metab. 99 (8) (2014) E1556–E1563.

[10] A.S. Weisberger, L.G. Suhrland, Studies on analogues of L-cysteine and L-cystine. II. The effect of selenium cystine on Murphy lymphosarcoma tumor cells in the rat, Blood 11 (1) (1956) 11–18.
[11] S. Kassam, et al., Methylseleninic acid inhibits HDAC activity in diffuse large B-cell lymphoma cell lines, Cancer Chemother. Pharmacol. 68 (3) (2011) 815–821.
[12] F. Hazane-Puch, et al., Sodium Selenite Decreased HDAC Activity, Cell Proliferation and Induced Apoptosis in Three Human Glioblastoma Cells, Anti-Cancer Agents Med. Chem. 16 (4) (2016) 490–500.
[13] N. Xiang, et al., Selenite reactivates silenced genes by modifying DNA methylation and histones in prostate cancer cells, Carcinogenesis 29 (11) (2008) 2175–2181.
[14] C. Hu, et al., Upregulation of KLF4 by methylseleninic acid in human esophageal squamous cell carcinoma cells: modification of histone H3 acetylation through HAT/HDAC interplay, Mol. Carcinog. 54 (10) (2015) 1051–1059.
[15] J.X. de Miranda, et al., Effects of selenium compounds on proliferation and epigenetic marks of breast cancer cells, J. Trace Elem. Med. Biol.: Organ Soc. Miner. Trace Elem. 28 (4) (2014) 486–491.
[16] A. Eriksson, A. Lennartsson, S. Lehmann, Epigenetic aberrations in acute myeloid leukemia: early key events during leukemogenesis, Exp. Hematol. 43 (8) (2015) 609–624.
[17] Y. Qu, et al., Cancer-specific changes in DNA methylation reveal aberrant silencing and activation of enhancers in leukemia, Blood 129 (7) (2017) e13–e25.
[18] M. Karimi, et al., LUMA (LUminometric Methylation Assay)–a high throughput method to the analysis of genomic DNA methylation, Exp. Cell Res. 312 (11) (2006) 1989–1995.
[19] J.S. Damiano, L.A. Hazlehurst, W.S. Dalton, Cell adhesion-mediated drug resistance (CAM-DR) protects the K562 chronic myelogenous leukemia cell line from apoptosis induced by BCR/ABL inhibition, cytotoxic drugs, and gamma-irradiation, Leukemia 15 (8) (2001) 1232–1239.
[20] X. Wu, et al., Determination of glutathione in apoptotic SMMC-7221 cells induced by xylitol selenite using capillary electrophoresis, Biotechnol. Lett. 38 (5) (2016) 761–766.
[21] P. Guo, et al., Preparation of two organoselenium compounds and their induction of apoptosis to SMMC-7221 cells, Biol. Trace Elem. Res. 154 (2) (2013) 304–311.
[22] C. Hu, et al., Upregulation of KLF4 by methylseleninic acid in human esophageal squamous cell carcinoma cells: modification of histone H3 acetylation through HAT/HDAC interplay, Mol. Carcinog. (2014).
[23] C.M. Weekley, et al., Selenite-mediated production of superoxide radical anions in A549 cancer cells is accompanied by a selective increase in SOD1 concentration, enhanced apoptosis and Se-Cu bonding, J. Biol. Inorg. Chem. 19 (6) (2014) 813–828.
[24] S. Kumar, M. Björnstedt, A. Holmgren, Selenite is a substrate for calf thymus thioredoxin reductase and thioredoxin and elicits a large non-stoichiometric oxidation of NADPH in the presence of oxygen, Eur. J. Biochem. 207 (2) (1992) 435–439.
[25] L. Guan, et al., P53 transcription-independent activity mediates selenite-induced acute promyelocytic leukemia NB4 cell apoptosis, BMB Rep. 41 (10) (2008) 745–750.
[26] P. Guo, et al., Preparation of a novel organoselenium compound and its anticancer effects on cervical cancer cell line HeLa, Biol. Trace Elem. Res. 151 (2) (2013) 301–306.
[27] C. Jiang, et al., Distinct effects of methylseleninic acid versus selenite on apoptosis, cell cycle, and protein kinase pathways in DU145 human prostate cancer cells, Mol. Cancer Ther. 1 (12) (2002) 1059–1066.
[28] R. Gowda, et al., Selenium-containing histone deacetylase inhibitors for melanoma management, Cancer Biol. Ther. 13 (9) (2012) 756–765.
[29] L. Galluzzi, et al., Molecular definitions of cell death subroutines: recommendations of the Nomenclature Committee on Cell Death 2012, Cell Death Differ. 19 (1) (2012) 107–120.
[30] N. Karelia, et al., Selenium-containing analogs of SAHA induce cytotoxicity in lung cancer cells, Bioorg. Med. Chem. Lett. 20 (22) (2010) 6816–6819.
[31] D. Desai, et al., SelSA, selenium analogs of SAHA as potent histone deacetylase inhibitors, Bioorg. Med. Chem. Lett. 20 (6) (2010) 2044–2047.
[32] H.J. Jung, Y.R. Seo, Current issues of selenium in cancer chemoprevention, BioFactors 36 (2) (2010) 153–158.
[33] M.P. Rayman, Selenium and human health, Lancet 379 (9822) (2012) 1256–1268.
[34] M.B. Meads, L.A. Hazlehurst, W.S. Dalton, The bone marrow microenvironment as a tumor sanctuary and contributor to drug resistance, Clin. Cancer Res. 14 (9) (2008) 2519–2526.
[35] S.M. Garrido, et al., Acute myeloid leukemia cells are protected from spontaneous and drug-induced apoptosis by direct contact with a human bone marrow stromal cell line (HS-5), Exp. Hematol. 29 (4) (2001) 448–457.
[36] D.J. Hughes, et al., Selenium status is associated with colorectal cancer risk in the European prospective investigation of cancer and nutrition cohort, Int. J. Cancer 136 (5) (2015) 1149–1161.
[37] R.J. Tressler, P.N. Belloni, G.L. Nicolson, Correlation of inhibition of adhesion of large cell lymphoma and hepatic sinusoidal endothelial cells by RGD-containing peptide polymers with metastatic potential: role of integrin-dependent and -independent adhesion mechanisms, Cancer Commun. 1 (1) (1989) 55–63.
[38] M. Weismann, et al., Integrin-mediated intracellular Ca2+ signaling in Jurkat T lymphocytes, J. Immunol. 158 (4) (1997) 1618–1627.
[39] X. Wu, et al., Regulation of the L-type calcium channel by alpha 5beta 1 integrin requires signaling between focal adhesion proteins, J. Biol. Chem. 276 (32) (2001) 30285–30292.
[40] Y. Wu, et al., Delineating the mechanism by which selenium deactivates Akt in prostate cancer cells, Mol. Cancer Ther. 5 (2) (2006) 246–252.
[41] M.E. Hemler, Tetraspanin functions and associated microdomains, Nat. Rev. Mol. Cell Biol. 6 (2005) 801–811.
[42] M. Furuya, et al., Down-regulation of CD9 in human ovarian carcinoma cell might contribute to peritoneal dissemination: morphologic alteration and reduced expression of??1 integrin subsets, Cancer Res. 65 (7) (2005) 2617–2625.
[43] J.C. Wang, et al., Down-regulation of CD9 expression during prostate carcinoma progression is associated with CD9 mRNA modifications, Clin. Cancer Res. 13 (8) (2007) 2354–2361.
[44] M. Zöller, Tetraspanins: push and pull in suppressing and promoting metastasis, Nat. Rev. Cancer 9 (1) (2009) 40–55.
[45] V. Gandemer, et al., Five distinct biological processes and 14 differentially expressed genes characterize TEL/AML1-positive leukemia, BMC Genom. 8 (2007) 385.
[46] V. Gandemer, et al., CD9 expression can be used to predict childhood TEL/AML1-positive acute lymphoblastic leukemia: proposal for an accelerated diagnostic flowchart, Leuk. Res. 34 (4) (2010) 430–437.
[47] M.P. Arnaud, et al., CD9, a key actor in the dissemination of lymphoblastic leukemia, modulating CXCR4-mediated migration via RAC1 signaling, Blood 126 (15) (2015) 1802–1812.
[48] H.-J. Tsai, C.-P. Tseng, The adaptor protein disabled-2: new insights into platelet biology and integrin signaling, Thromb. J. 14 (Suppl 1) (2016) 28.
[49] C.P. Tseng, et al., Disabled-2 small interfering RNA modulates cellular adhesive function and MAPK activity during megakaryocytic differentiation of K562 cells, FEBS Lett. 541 (1–3) (2003) 21–27.
[50] S.R. Majeed, et al., Clathrin light chains are required for the gyrating-clathrin recycling pathway and thereby promote cell migration, Nat. Commun. 5 (2014) 3891.
[51] A. Mai, et al., Distinct c-Met activation mechanisms induce cell rounding or invasion through pathways involving integrins, RhoA and HIP1, J. Cell Sci. 127 (Pt 9) (2014) 1938–1952.
[52] M.R. Akl, et al., Molecular and clinical profiles of syndecan-1 in solid and hematological cancer for prognosis and precision medicine, Oncotarget 6 (30) (2015) 28693–28715.
[53] J. Zhou, J.T. Hsieh, The inhibitory role of DOC-2/DAB2 in growth factor receptor-mediated signal cascade. DOC-2/DAB2-mediated inhibition of ERK phosphorylation via binding to Grb2, J. Biol. Chem. 276 (30) (2001) 27793–27798.
[54] S.M. Cheong, et al., Dab2 is pivotal for endothelial cell migration by mediating VEGF expression in cancer cells, Exp. Cell Res. 318 (5) (2012) 550–557.
[55] B.A. Hocevar, et al., The adaptor molecule Disabled-2 links the transforming growth factor beta receptors to the Smad pathway, EMBO J. 20 (11) (2001) 2789–2801.
[56] C.P. Tseng, et al., Induction of disabled-2 gene during megakaryocyte differentiation of k562 cells, Biochem. Biophys. Res. Commun. 285 (1) (2001) 129–135.
[57] C.L. Huang, et al., Disabled-2 is a novel alphaIIb-integrin-binding protein that negatively regulates platelet-fibrinogen interactions and platelet aggregation, J. Cell Sci. 119 (Pt 21) (2006) 4420–4430.
[58] S. Waelter, et al., The huntingtin interacting protein HIP1 is a clathrin and alpha-adaptin-binding protein involved in receptor-mediated endocytosis, Hum. Mol. Genet. 10 (17) (2001) 1807–1817.
[59] L. Chen, et al., Both mTORC1 and mTORC2 are involved in the regulation of cell adhesion, Oncotarget 6 (9) (2015) 7136–7150.
[60] A. Riaz, K.S. Zeller, S. Johansson, Receptor-specific mechanisms regulate phosphorylation of AKT at Ser473: role of RICTOR in beta1 integrin-mediated cell survival, PLoS One 7 (2) (2012) e32081.